Journal of Ecology 1995, **83**, 497–507

A model simulating the genesis of banded vegetation patterns in Niger

J. M. THIÉRY, J.-M. D'HERBÈS* and C. VALENTIN*

*CEA/DPVE, Centre de Cadarache, 13108 Saint-Paul-lez-Durance, France and *ORSTOM, B.P. 11416, Niamey, Niger*

Summary

1 Two-phase mosaics, or striped vegetation patterns (densely vegetated bands alternating regularly with bare areas), have been reported in arid and semiarid zones. They can occur provided (a) total rainfall is not sufficient to maintain a dense cover; and (b) sufficient and uniform sheet flow can compensate, at least partly, for the lack of water.

2 Recent studies demonstrate that vegetation bands follow a successional model, in which bare areas are colonized by a *pioneer front*. Local studies in South West Niger suggest that transitions could occur between the various patterns observed within the same ecological region, but with varying average rainfall and surface features.

3 Because these transitions could not be followed in the field without long term studies, a simple model has been elaborated to simulate the different structures observed. This model, based on cellular automata, is derived from the '*game of life*' and depends only on two hypotheses which reflect *competition* and *synergy*: the establishment, growth and survival of a given plant will be affected *negatively* by the influence of plants situated up-slope and *positively* by lateral and down-slope plants.

4 A matrix with 9×3 elements is applied to the same initial tree distribution grid, with three values of the a coefficient reflecting up-slope resource competition and two values of b reflecting lateral synergies.

5 The results demonstrate that almost all the structures observed in the field can be generated by this simple model, by varying only the two parameters a and b and the number of iterations. This result is independent of the initial tree density, showing that observed structures could equally well be derived from more or less dense vegetation patterns.

Keywords: '*brousse tigrée*', cellular automata, competition, Sahel, sheet flow

Journal of Ecology 1995, **83**, 497–507

Introduction

Much of the current interest in landscape ecology stems from the central concept that if landscape structure can direct water and nutrient flows, then ecological processes can in turn modify the landscape structure. In semiarid and arid zones, the landscape imposes constraints on the orientation and rates of these flows. In response to such constraints, the vegetation cover tends to contract and to produce specific patterns, which may, in return, affect the behaviour of the functional landscape units.

Such feedbacks were recently illustrated by the study of the dynamics of vegetation bands in Northern Mexico (Cornet *et al.* 1988; Cornet *et al.* 1992; Montaña *et al.* 1990; Montaña 1992). This vegetation pattern consists of alternating arcs of vegetation and bands of bare ground, generally on gentle slopes (less than 0.6°). Sheet run-off generated on the bare patches between the arcs accumulates and infiltrates at the upper edge of an arc. This additional soil moisture, induced by the landscape structure, facilitates plant colonization of the leading edge of the arc, and hence there is a continual migration of vegetation arcs across the landscape.

Equivalent processes have often been suggested to explain the maintenance of similar vegetation patterns in other areas, such as '*brousse tigrée*' (Fig. 1) in French-speaking West Africa (Clos-Arceduc 1956; White 1971; Ambouta 1984; Serpantié *et al.* 1991), '*tiger bush*' in East Africa (Worrall 1959; Boaler & Hodge 1962, 1964; Hemming 1965; Wickens & Collier

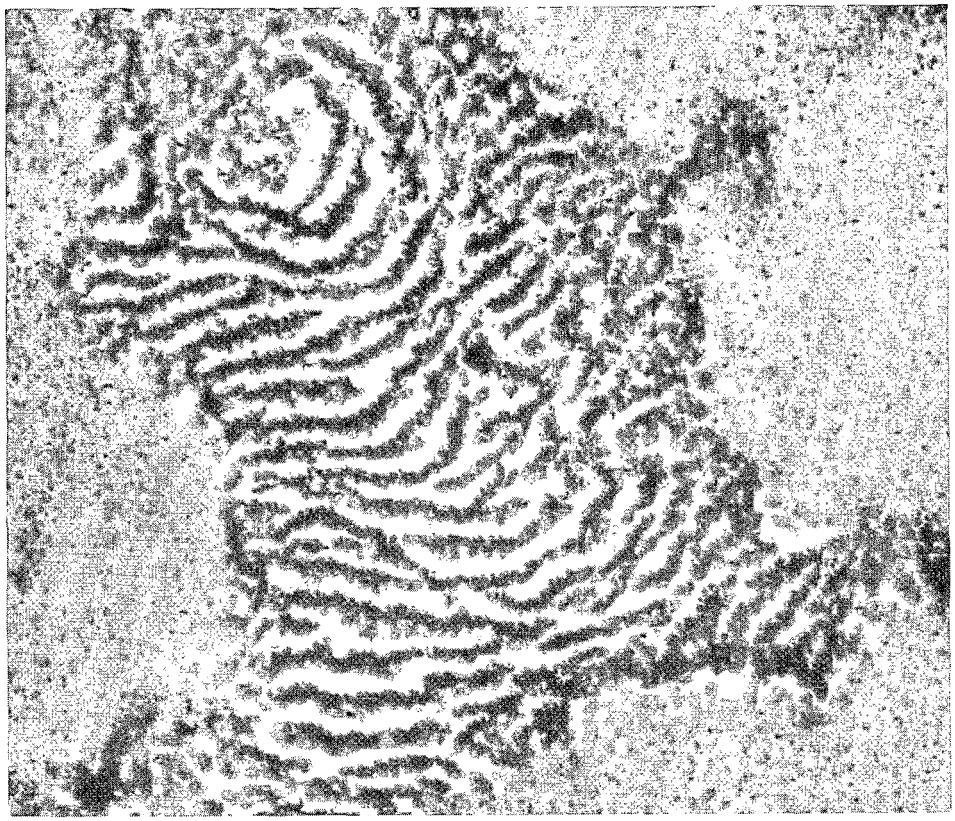

Fig. 1 Aerial view of a plateau with a well-developed '*brousse tigrée*' pattern in South West Niger (13°30'N; 2°40'E). The picture sizes are approximately 2.4 by 2 km.

1971), '*striped vegetation pattern*' in South Africa (Van der Meulen & Morris 1979), and '*grove-intergrove pattern*' in Australia (Mabbutt & Fanning 1987; Tongway & Ludwig 1990). A simulation model based on waterflows was recently proposed (Mauchamp *et al.* 1994); however, the vegetation arcs in Jordan (White 1969) and in Mali (Leprun 1992) were reported to be perpendicular to the direction of the dominant wind, suggesting that wind could be also a crucial factor. Whatever the prevailing factor claimed for the maintenance and the possible migration of the arcs, the crucial question of how such patterns originate has yet to be clearly elucidated. The most common hypotheses suggest either the gradual degradation of an originally uniform plant cover due to climatic or soil degradation (White 1971), or conversely, the colonization of previously bare zones (Boudet 1972). A subsidiary question arises as to whether some less structured patterns can be identified as primary banding patterns.

The vegetation patterns observed in the plateaux of South West Niger suggest that spatial transitions could reflect temporal successions between more or less structured patterns. However, given the inherent difficulties of long-term field experiments, simulation modelling appears a good alternative for providing some insights into this question. Can the succession of bush savannah patterns prior to the establishment of a '*brousse tigrée*' pattern be both simulated and recognized in the field ? The proposed cellular automata model, derived from the '*game of life*' (Conway 1976), is based on simple hypotheses about negative (*competitive*) and positive (*synergistic*) interactions between individuals.

The objectives of this study are (a) to evaluate the validity of the simulation model in terms of landscape ecology (b) to put forward new hypotheses on temporal and spatial relationships between the typical '*brousse tigrée*' and other neighbouring vegetation patterns.

Materials and methods

THE STUDY AREA

South West Niger, in the region of its capital Niamey, encompasses four major geomorphologic elements (Wilding & Daniels 1989): (1) broad ironstone-capped plateaux with slopes generally lower than 0.3° (2) sand valley systems that slope gently from the plateaux toward a dry stream bed (3) broad terrace-like sand plains, and (4) fossil valleys ('*dallols*').

Major plateaux, several kilometres broad, occur at elevation of 220–240 and 260 m a.s.l. They comprise 23% of the area surveyed and are locally covered by thin aeolian sands, with or without low dune forms, similar to those in valley systems.

Annual rainfall in the Niamey region (mean for 1968–89 = 496 mm) varies greatly from year to year, and for the past 20 years has been considerably lower

than the 80-year average (mean for 1905–89 = 560 mm; Lebel *et al.* 1992). Rainfall distribution is unimodal, usually starting in June, after an intensive dry period, and lasting until early September. Rainfall comes generally in the form of high-intensity storms. The hottest period is in April–May.

Land in this Sahelian region is used mainly for millet culture on the aeolian sandy deposits over the four geomorphologic elements, and for cattle, sheep and goat grazing. Most of the wood used for domestic energy is collected from the plateaux and in the fallow fields.

Studies were carried out at two levels. A general survey was conducted to produce a map of surface conditions, at the scale 1/200 000, of the '*square degree*' (i.e. 1° latitude by 1° longitude) around Niamey (2–3°E, and 13–14°N). In addition, a 20 km × 20 km research site was established, about 75 km east of Niamey, to initiate more detailed studies (Goutorbe *et al.* 1994).

BANDED VEGETATION PATTERNS IN SOUTH WEST NIGER

Distribution and characterization

The '*brousse tigrée*' pattern, which covers an area estimated at 22 000 km^2 (Ambouta 1984), occurs in this region only on the plateaux.

The soils of the laterite-capped plateaux are thin and poorly developed, over a laterite gravel and sesquioxide sheet (petroferric) contact. The fairly uniform substratum of these soils consists of highly weathered materials of loamy Continental Terminal deposits, locally overlaid by aeolian sand derived from these sediments. In general, these soils exhibit between 25 and 85 cm of gravely loam cover materials over cemented sesquioxide sheets or ironstone gravel. Most of these soils are Ustoxic Dystropepts. Kaolinite is the prevailing clay mineral. These acidic soils (pH < 5.0) have very low nutrient reserves (cation exchange capacity < 70 meq kg^{-1}; Ambouta 1984) and low water storage capacity owing to their shallow depth and high coarse fragment content (pebble and gravel).

The bush vegetation in the area is dominated by Combretaceae. The '*brousse tigrée*' pattern is located between 13°N and 15°N (Gavaud 1966), i.e. in a region where average annual rainfall decreases steeply from 750 mm down to 400 mm, from south to north. The width of both the woodland bands and the associated bare lanes increases from south to north (Gavaud 1966).

Structure

The characteristics of a '*brousse tigrée*' pattern were determined by sampling systematically along a 74-m transect perpendicular to the bands in a typical region (13°33'N). This transect (see Fig. 2) started in the down-slope portion of a band, crossed the barren area, into the leading edge of the next band, and stopped at the boundary of its down-slope portion. Surface features, noted in every consecutive 1-m × 1-m quadrat, were: percentage plant cover; the dominant species in the tree, shrub and grass layers; the litter on soil surface (type, percentage cover); microrelief features (i.e. microsteps, shallow rills, gravel micromounds); termite mounds and surface harvesting tunnels; large macropores open at surface; various crust types as defined in the hydrological classification of Casenave & Valentin (1992), and the type and severity of run-off and erosion features. In addition, two soil profiles were taken, one from the band and one from the interband areas.

The characteristics of this '*brousse tigrée*' pattern are very similar to those reported by White (1970) and Ambouta (1984) in the same region, and confirmed during an extensive mapping of the study area (Goutorbe *et al.* 1994).

The transect (i.e. band + interband) could be divided into five typical zones (Fig. 2).

(1) *The Degraded zone* (*D*) in the lower sector of the upper band (0–8 m). Shrub cover drops from 40 to 0%, whilst the proportion of dead shrubs increases

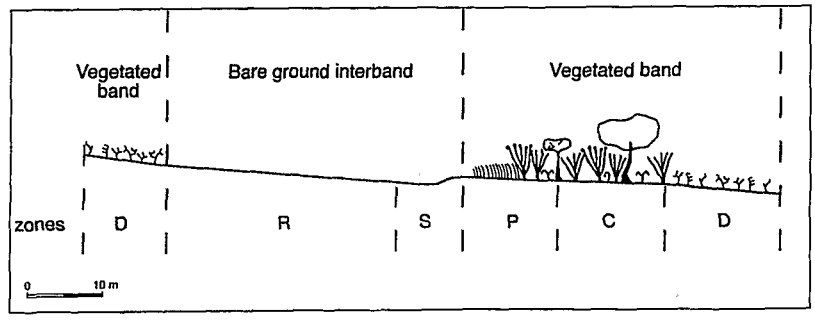

Fig. 2 Schematic cross-section of a '*brousse tigrée*' showing the different zones: D (Degraded), R (Run-off), S (Sedimentation), P (Pioneer front), C (Central, or Close bush). The transect described in the article starts with the up-slope D-zone and finishes with the C-zone.

dramatically up to 100%. This layer consists of *Combretum micranthum* G. Don., *Boscia angustifolia* A. Rich. and *B. senegalensis* (Pers.) Lam. ex Poir. The ground surface is sparsely covered by shrub residues. More than half of the surface is occupied by structural crusts. These sieving crusts associated with gravel crusts indicate intensive sheet flow (Valentin & Bresson 1992). Abandoned termite mounds, mainly of *Macrotermes subhyalinus,* occur in this bottom edge of the band.

(2) *The Run-off zone* (*R*) in the upper and median sector of the interband (9–36 m) has no plant cover. Although abandoned termite mounds (mainly of *Odontermes*) may occur, there are no active termite constructions. The erosion crusts (characterized by a smooth hard surface) and the gravel crusts produce an intensive run-off. There are no linear incisions to indicate any distinct concentration of sheet flow.

(3) *The Sedimentation zone* (*S*) in the lower sector of the interband (37–41 m). Also bare of vegetation and termite activity, this belt is characterized by sedimentary crusts which spread over nearly the whole surface, thus covering erosion and gravel crusts. These sedimentary crusts usually crack and may form typical curled plates.

(4) *The Pioneer front zone* (*P*) in the upper sector of the next band (42–45 m). Local concavities, or '*bays*', and salients, or '*capes*', are found at the boundary with the previous zone. The bays are associated with a nearly total cover of annual grasses (*Zornia glochidiatia* Reichenb. ex DC., *Monechma ciliatum* (Jacq.) Milne-Redh., *Schoenefeldia gracilis* Kunth.) whilst the capes are predominantly colonized, chiefly vegetatively, by the shrub *Guiera senegalensis*. In both situations, the sedimentary crusts are almost entirely destroyed by plant emergence and termite activity (*Macrotermes subhyalinus*, *Cubitermes* spp., and *Procubitermes* spp.)

(5) *The Central zone* (*C*) in the middle of the band (46–74 m). Canopy cover ranges between 60 and 100%. The upper region is predominantly occupied by *Guiera senegalensis*, which is progressively replaced by *Combretum micranthum* further down the slope. Taller trees, up to 8 m, commonly including *Combretum micranthum*, *C. nigricans* Lepr. ex Guill., *C. glutinosum* Perr. ex DC., *Cassia sieberiana* DC., *Acacia ataxacantha* DC., *A. macrostachya* Reichenb. ex Benth. and *Sclerocarya birrea* (A. Rich.) Hochst. occur only in the lower part of this zone. An understorey of small shrubs, mainly *Gardenia sokotoensis* Stapf. et Hutch. and some lianas (*Grewia flavescens* Juss.), provides a minor component of the cover (10%). Grass cover is very sparse (< 5%). Under the thick vegetation litter (3–5 cm thick, 80% of ground cover), the soil surface has high porosity, mainly induced by termite activity. Surface crusts are virtually absent apart from a few remnants of sedimentary crusts, colonized by algae, and erosion crusts are restricted to the vicinity of active termite mounds. The boundary with the lower sector (D) of the band is very abrupt (< 2 m).

Soils

Soils in and between the vegetation bands showed few morphological differences, apart from those which can be directly accounted for by the influence of the vegetation itself (i.e. higher porosity and rooting within the band). These observations are consistent with those of Barker (1992) who studied 40 pits in five transects across bands and interbands, also in South West Niger, and concluded that a slight increase in soil depth (15–20 cm) in some band soils compared to interband soils was presumably due to the high level of root activity and prolonged wetting. The main differences between the two soils occur in the 0–20 cm top layer (Ambouta 1984); in the band, organic matter content (0.71% C) is higher than in the interband (0.27% C), but clay content is lower (17% instead of 33%). As a result, exchangeable cation concentration, albeit greater in the band (18 vs. 10 meq kg^{-1} in the interband), was extremely low.

The iron cap is poorly fragmented but allows deep infiltration and rooting in the Continental Terminal deposits. Old roots have been found in all zones, including the Run-off zone (Barker 1992).

Slope profile and hydrological processes

The overall transect slope was 0.3°. Maximum local slopes recorded during topographic surveys (Ambouta 1984) ranged between 0.9° in the bands and 1.4° in the interbands. The general topographic profile therefore presents a step-like profile with the steepest mean slope in the degraded (D) zone of the vegetation band and the lowest slope in its pioneer front (P) and central (C) zones, with a frequent slight counter-slope in the lower sedimentary zone of the interband (S, Fig. 2), probably due to several processes. In addition to the gradual trapping of sediments yielded by sheet flow and the accumulation of plant residues, the higher sand content in the band than in the interband suggests incorporation of aeolian deposits. Termite activity may also be important as it raises material from deep horizons as well as it increases soil porosity. Such a damming is responsible for up-slope ponding, hence for the occurrence of sedimentary crusts

Run-off and run-on were simulated using an hydrological model based upon the classification of surface features (Casenave *et al.* 1992). On a yearly basis, the core of the vegetation band is expected to intercept a run-on amount approximately equal to the rainfall amount.

Dynamic hypotheses

The surface features of the '*brousse tigrée*' pattern tend to corroborate the occurrence of a slow up-slope

migration. It is hypothesized that when plants colonize the upper part of the vegetation band, they gradually reduce resources for the rest of the band and consequently, the whole band should tend to move upward (as in Sudan grass patterns, Worrall 1959). This assumption is supported by the temporal succession of different crusts along the transect, which is consistent with that proposed by Valentin *et al.* (1992).

First, the down-slope edge (D) of the band decays when conditions become too moisture deficient to maintain a dense vegetation cover. This implies that run-on from the interband area is most frequently absorbed by the pioneer front (P) and the central zone (C) of the band, though some may pass through the entire band when intense storms occur on already nearly saturated soils. This decline in vegetation cover results in decreased litter production, exposing soil to the beating actions of raindrops, so that structural crusts develop and remain unaltered due to reduced termite activity. Such conditions maximize run-off.

Second, the removal of the upper sandy layers of the structural crust leading to the expansion of erosion crusts can be ascribed partly to increased sheet run-off conditions, partly to deflation enhanced by the vegetation collapse. In this latter case, sand is presumably trapped by the surrounding bands of vegetation, which would explain the enrichment in the sand fraction under bands. Wherever erosion accelerates so as to expose the gravelly layer, initial structural and erosion crusts are gradually altered into gravel crusts. Erosion and gravel crusts generate an intense run-off, but tend to protect the soil from further degradation, provided sheet flow does not concentrate (Casenave *et al.* 1992). The gradual accumulation of sediments tends to even the land surface, with sedimentary crusts increasingly covering the erosion and gravel crusts. This silting of small depressions fosters the slow encroaching of the temporary flooded areas over the bare lane. The whole '*brousse tigrée*' pattern can be considered therefore as a typical erosion-deposition sequence through space and time.

Third, colonization of sedimentary crusts by grass and by layering pioneer shrubs is greatly fostered by the cracks. Furthermore, the sedimentation zone (S) intercepts run-on, sediments, and seeds removed by surface flow or wind from the bare interband, as observed in the sediments.

Fourth, owing to the favourable moist conditions, succession in time and space is then observed through the band from the youngest pioneer plants at the leading edge (grass species and *Guiera senegalensis*) to the older and more water-demanding trees as *Combretum* spp. in the central zone (C). When the distance from the catchment source increases as a consequence of the slow up-slope shift of the band, the vegetation decays and the cycle starts again.

The model

MODEL DESCRIPTION

We use a cellular automata formalism similar to the one introduced by Conway (1976) as the '*Game of life*' (Delahaye 1991). We assume that each tree can only grow on predefined sites located on a regular grid and that one tree species is dominant. All trees are equivalent but may have different states corresponding to different metabolic characteristics (e.g. photosynthetic activities). If we assume only four states for a tree in a given site, *State 0* could indicate a site with no tree (or with a dead tree), *State 1* could indicate a young tree (or a senescent tree), *State 2* a small tree or a stressed adult tree, and *State 3* a well watered adult tree. State number therefore represents the tree performance, rather than its age or its size.

The '*brousse tigrée*' is described by a state matrix, representing the tree state on each site, at a given time. This state matrix could be obtained by digitizing an aerial infra-red picture. Each site would correspond to one picture element (pixel) rather than to one tree, and the state to the colour level, i.e. to the local tree performance. With this interpretation, the site size may have any value (e.g. 1–10 m) depending on the picture resolution.

To follow the dynamics of such a model, we have to make hypotheses on transitions between states. Like Conway, we assume that changes in the $S_{i,j,k+1}$ state (at site ij at iteration $k+1$) depend only on the states of the neighbouring sites at iteration k. The original *Game of life* was completely isotropic and the sum of adjacent states was taken as an index for local population density, triggering birth (normal population) or death (over-population). In the present model, we weight each site by a convolution matrix which represents *competition* (negative weights) or *synergy* (positive weights).

For example, for each site (labelled by a star *), the convolution matrix $C_{m,n}$ represents the effects of its neighbouring sites, e.g.

$$\begin{matrix} -1 & -2 & -1 \\ 0 & -1 & 0 \\ 1 & * & 1 \\ 1 & 1 & 1 \end{matrix} \qquad (1)$$

This matrix introduces two hypotheses:

1 that plants situated directly up-slope, and to a lesser extent diagonally up-slope, hamper the establishment, growth and survival of the labelled plant; and
2 that lateral and down-slope plants have a positive influence on the establishment, growth and survival of the labelled plant.

The first hypothesis stems from the unidirectional pattern of flow, i.e. down-slope. The second hypothesis is strongly supported by the observations that dense vegetation tends to create its own favourable

environment. Factors include micropedoclimatic changes due to shading, accumulation of vegetation litter, root penetration and soil deepening, faunal activity, reduced crusting, improved infiltrability and higher water storage. Both hypotheses are thus mainly related to water resource availability and competition.

By weighting all the neighbouring states, we may obtain large positive or negative numbers leading to large state changes, which could be unrealistic. Even under very favourable conditions, a tree cannot grow faster than allowed by its own phenology. We introduce a lower limit B and a higher limit H on state changes (usually -1 and $+1$). We also introduce a calibration factor c which allows an empirical fit of the transition probabilities.

The transition formula is:

$$S_{i,j,k+1} = S_{i,j,k} + Max(B, Min(H, c\,\Sigma_{m,n}\, C_{m,n}\, S_{i+m,j+n,k})), \quad (2)$$

where the m and n indices run over all the non zero lines and columns of the $C_{m,n}$ convolution matrix. This formula can be easily understood from matrix 1 (with $B = -1$, $H = 1$, and $c = 1$): for a site ij surrounded by a nearest neighbour site X in state 2 (all other sites being in state 0)

$$S_{i,j,k+1} = S_{i,j,k} + Max(-1, Min(1, -1 * 2)) = S_{i,j,k} - 1 \quad (3)$$

for the *up-slope* site X, and

$$S_{i,j,k+1} = S_{i,j,k} + Max(-1, Min(1, 1 * 2)) = S_{i,j,k} + 1, \quad (4)$$

for the *down-slope* site X.

For a complete simulation, we have to assume an initial state matrix $S_{i,j,0}$. We could have used aerial pictures taken in the past (e.g. around 1960). But for preliminary simulations, random initial pictures are more convenient and introduce no statistical bias.

Model implementation

The °*TIGREE*° model was written with the °*VOYONS*° general purpose modelling software (Thiéry 1991). This °*VOYONS*° application runs on standard PCs (mathematical coprocessors are recommended) and is available on request (e-mail: thiery@orstom.orstom.fr). Only two specific subroutines were added, one for the fast computation of local interactions and one for the graphical display of tree-like symbols.

Computations should be run on very large matrices in order to reduce eventual border effects. In °*TIGREE*°, we assume periodical conditions which are often used in crystallography or solid state physics. The *left neighbour* of a plant in column 1 is on the same line in the last column; the *up-slope neighbour* of a plant in the first line is on the last line.

Results

Once started, the °*TIGREE*° model is completely deterministic: for a given initial condition, the final result depends only on the convolution matrix and on the number of iterations. Preliminary computations were run with many different matrices: simple 3×3 matrices or 4×3 matrices (as matrix 1) are sufficient to see the general results but more realistic pictures obtain with larger matrices (e.g. 9×3 matrices with potentially 27 independent elements). In order to simplify the discussion we have assumed that the matrix elements were strongly correlated and the results will be presented for the convolution matrix (5):

$$\begin{matrix} 0 & -a & 0 \\ 0 & -a & 0 \\ 0 & -a & 0 \\ 0 & -a & 0 \\ 0 & -a & 0 \\ 0 & -a & 0 \\ b & * & b \\ 0 & 3 & 0 \\ 0 & 1 & 0 \end{matrix} \quad (5)$$

This convolution matrix depends on only two parameters a and b, where a represents the *up-slope competitions* of hypothesis 1, and b the *lateral synergies* of hypothesis 2. These two unitless coefficients are calibrated against the *down-slope synergies*, e.g. b is equal to the relative value of the lateral synergy compared to the down-slope synergy. More precisely, when $b = 1$, a lateral neighbour site has the same effect as the down-slope next-neighbour site and similarly, when $a = 1$, an up-slope site has the opposite effect of the down-slope next-neighbour site (in this matrix, the down-slope neighbour site is three times more effective than the down-slope next-neighbour site).

Inspection of the convolution formula (eqn 2) indicates that, in order to generate transitions between $S_{i,j,k}$ *states, the calibration factor* c should not be too small. Conversely, too large a calibration factor will generate too many transitions, which will be unrealistic. These *a priori* conclusions were confirmed by preliminary computations and all results in this article are presented for a calibration factor $c = 0.4$.

Figure 3 displays the simulation results after 1, 4 and 20 iterations, starting always with the same random state distribution (with a cover density equal to 0.30, i.e. with 30% of occupied sites). A large variety of images can be obtained by varying only two parameters. These images reproduce many patterns observed on aerial photographs (e.g. Figs 1 and 4), and include Y type patterns (Case D20) and isolated islands (Case E20). Tree clustering in long bands appears after 20 iterations under favourable conditions (Case D20), whereas 100 iterations are necessary to produce such banding when large up-slope competitions and small lateral synergies are imposed.

For a more quantitative discussion, we have com-

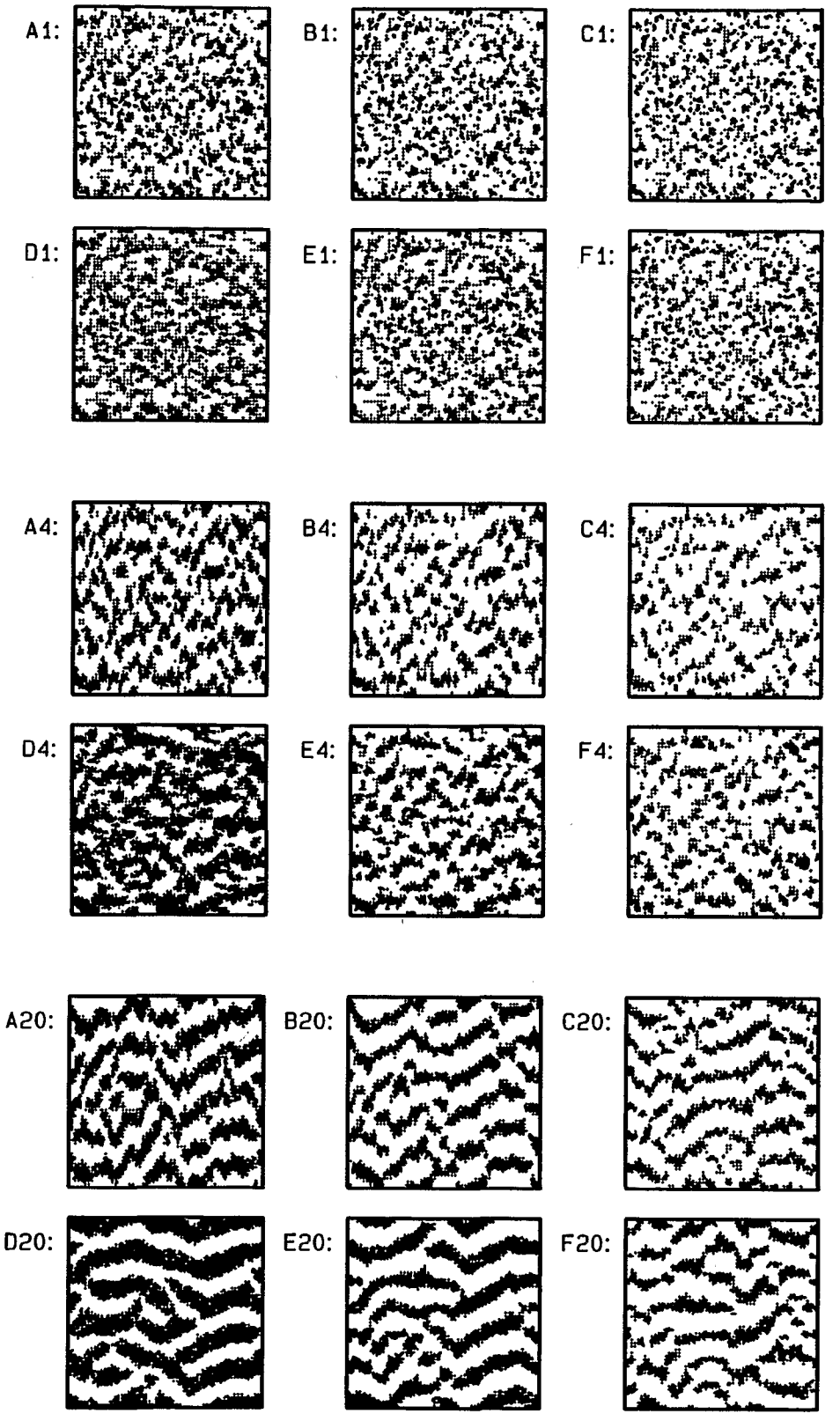

Fig. 3 Patterns generated by the model with various parameter values: $a = 2$ (A, D), 4 (B, E) or 8 (C, F); $b = 1$ (A, B, C) or 4 (D, E, F). The iteration number ($k = 1$, 4 or 20) is proportional to time and should be calibrated against experimental data (see Discussion). Vegetation is represented by random tree-like symbols with a size proportional to the state variable.

puted many statistical results such as the density of sites in state i, the density of empty sites (or *desert density*) and the complementary density of occupied sites (or *cover density*). In order to quantify the banding process, we have introduced the notion of *group*, a series of at least two neighbouring occupied sites

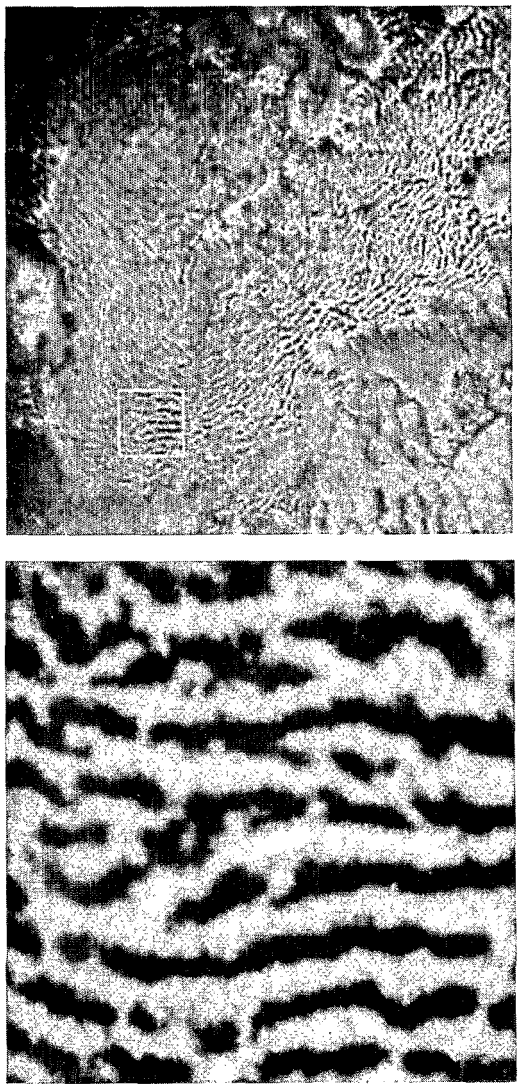

Fig. 4 Scanned aerial picture of a plateau in the region of Niamey (a) (5 km × 5 km) and a local enlargement (b) (650 m × 650 m) showing a well-designed band pattern comparable to the simulation D20 in Fig. 3.

lying on the same vertical line for a least two iterations. Groups are dynamic patterns which may appear, survive, or disappear. Occupied sites which are not in a group are considered as *isolated*. A *cluster* is a series of adjacent vertical groups, while *bands* represent clusters extended on many horizontal sites (e.g. case C4 of Fig. 3 presents many small clusters which cannot be considered as true bands).

The program can easily recognize all groups lying on one vertical pixel line and computes parameters such as their *width* (number of occupied pixels) or their *velocity* (change in the position of the centre of gravity between two iterations). The *group width* is defined vertically as an estimation of the band width. Table 1 displays some of these parameters averaged over all vertical lines, for the cases represented in Fig. 3.

Table 1 focuses on the *grouping effect* rather than on the *banding process*, which cannot easily be quantified. The computer band analysis would require elaborate pattern recognition algorithms, especially with Y shaped bands (e.g. D20, Fig. 3) or with merging bands. In most cases group statistics should give good estimates of band statistics, except for low density pictures where detailed analyses should distinguish between cluster statistics and true band statistics (e.g. C4, Fig. 3). For high resolution digitized pictures, group statistics can be more rapidly computed than the corresponding band statistics.

Results in Table 1 are not completely independent: e.g. the product of the *mean group number* and the *mean group width* is equal to the product of the *group density* and the *number of vertical pixels*. All density terms are by definition correlated.

All results vary with a and b parameters but not to the same degree. The *mean group number* (an estimate of the *averaged band number*) converges toward 5.1–5.6 after only 20 iterations. The *mean group width* decreases strongly (e.g. from 5.8 in D20 to 3.5 in *F*20), when a increases. It increases slightly when b increases. Similar variations obtain for the *cover density*. These numerical results can be easily interpreted. The model predicts a nearly constant *averaged band number*, i.e. a nearly constant *band+interband width*. The *band width* decreases strongly when the competition increases and increases slightly with the lateral synergy.

Discussion

In an attempt to validate the model, aerial photographs (such as Fig. 4) were scanned and compared with the maps originated by the model (Fig. 3). Some differences can be observed in the relative proportions of bands and interbands, but, as pointed out by Gavaud (1966), these characters depend mainly upon the mean annual rainfall. Vegetation bands appear either as straight lines, or in the form of concentric arcs, suggesting a slight convex topography of the plateaux.

Some frequently observed distinctive patterns (e.g. intersecting and branching vegetation lines, Figs 1 and 4) appeared in the simulations at the onset of vegetation banding. Such patterns might be therefore considered as intergrades between initial clusters established accidentally and mature vegetation bands running along contour lines. According to the model, plant clusters occurring at random, possibly as a response to local accidents such as termite mounds (Boaler & Hodge 1964; White 1971), tend gradually to form a vegetation line oriented perpendicular to the direction of run-off. Observed reticulations would result from such transitory banding stages rather than from criss-cross patterns of sheet flow as proposed by Mabbutt & Fanning (1987).

With the notable exception of the initial stages, bands generated by the model extend as far as the border of the map (or the window). This does not

Table 1 Statistical results computed for the different patterns displayed in Fig. 3. Group statistics (mean group number, mean group width and group density) are estimates of band statistics (see text)

Cases	a	b	Mean group number	Mean group width	Group density	Isolated site density	Cover density	Desert density	Mean velocity
A1	2	1	5.893	2.973	0.313	0.060	0.373	0.627	0.469
B1	4	1	4.429	2.762	0.218	0.092	0.310	0.690	0.328
C1	8	1	3.607	2.644	0.170	0.107	0.277	0.723	0.269
A4	2	1	5.304	4.249	0.402	0.009	0.411	0.589	0.636
B4	4	1	4.625	3.490	0.288	0.017	0.305	0.695	0.773
C4	8	1	3.893	2.917	0.203	0.031	0.234	0.766	0.905
A20	2	1	5.089	5.274	0.479	0.002	0.481	0.519	0.715
B20	4	1	5.393	4.073	0.392	0.002	0.394	0.606	0.685
C20	8	1	5.232	3.143	0.294	0.017	0.311	0.689	0.636
D1	2	4	7.196	3.588	0.461	0.074	0.535	0.465	0.543
E1	4	4	5.518	3.032	0.299	0.093	0.392	0.608	0.421
F1	8	4	4.179	2.739	0.204	0.108	0.312	0.688	0.316
D4	2	4	6.982	4.248	0.530	0.035	0.565	0.435	0.243
E4	4	4	5.607	3.252	0.326	0.041	0.367	0.633	0.420
F4	8	4	4.625	3.023	0.250	0.039	0.289	0.711	0.637
D20	2	4	5.393	5.825	0.561	0.002	0.563	0.437	0.382
E20	4	4	5.607	4.315	0.432	0.001	0.433	0.567	0.436
F20	8	4	5.125	3.453	0.316	0.019	0.335	0.665	0.511

happen in the field, where the bands are fragmented and allow direct connection between successive interbands. However, the model suggests that the individual segments tend to interconnect with each other, particularly as a response to the constraints imposed by lateral synergy. The frequent failure of such merging might be ascribed to locally adverse conditions, such as very serious crusting (gravel crusts) or concentrated run-off, which inhibit colonization of the bands ends. Although the up-slope colonization has been well documented, these lateral ecotones have not yet been investigated. The disruptions between arcs are too common to be initiated merely by cattle tracks.

Since a clear up-slope migration of the vegetation bands was simulated by the model, pattern changes are expected at the top of the landscape where bands do converge. In the field, decaying arcs abut against flat and barren areas (e.g. the '*eye*' at the top of Fig. 1). Such areas are suspected to produce insufficient sheet flow to maintain banding patterns.

The model could be adapted to allow for temporal variation in water resource availability by the introduction of a time dependent (i.e. an iteration dependent) coefficient $a(k)$. Under such erratic climatic conditions, the up-slope migration of band-interband systems is expected to be a discontinuous process. These changes could be simulated on Fig. 3 by shifts between Ck and Ak (or Fk and Dk). A succession of years of high rainfall would favour the thickening of the vegetation band, mainly through the accelerated colonization of the barren lane at the up-slope edge of the band and by a delayed decay of the bottom edge of the band. On the other hand, a prolonged drought period would accelerate decay of the bottom edge, widening the down-slope barren lane. As a result, increased amount of run-on would possibly compensate, at least partly, for the rainfall deficiency, stabilising the leading edge of the vegetation band. The net result of these alternating periods of above and below average rainfall would again be a continuous up-slope migration of vegetation bands.

Although this dynamic scheme has considerable appeal, only limited empirical data are presently available to judge its validity. The evolution of a '*brousse tigrée*' pattern was studied in a sparsely populated region of Burkina Faso, comparing aerial photographs taken in 1952 and 1984 (Serpantié *et al.* 1991). This study showed a clear maintenance of the pattern despite the fact that vegetation cover had decreased from 50 to 33%, as a result of drought. However, no conspicuous migration of bands was demonstrated. To our knowledge, the only field evidence of band shifts was recently given by Leprun (1992) in Mali, where a concrete geographical bench-mark installed in 1955 in a band was found 21 years later in a barren lane 15.8 m from the band. This migration gives a mean annual velocity of 0.75 m year^{-1}. Other bench-marks in the same region indicated annual velocities ranging between 0.20 and 0.25 m year^{-1}. Because this type of '*brousse tigrée*' pattern was mainly wind-controlled, these features cannot be necessarily extrapolated to sheet-flow dependent banding patterns, where the velocity could be slower. For grass patterns in Sudan, Worrall (1959) measured annual encroachments varying from 0.3–1.5 m year^{-1}.

The model indicates that banding can develop from various initial patterns, leading to a number of possible intergrades between such initial patterns and the final banding patterns. Recognition of these intergrades in relation to their location may lead to a better

understanding of banding processes in general. Such relationships need to be considered across large space- and time-scales. At the southern margin of the '*brousse tigrée*' region in Niger, similar plateau habitats are usually covered by a mosaic of bare ground and woodland patches. Such a vegetation arrangement is similar to the initial patterns which appeared in the model (e.g. A1 or D1, Fig. 3), when banding would occur as a response of the initial mosaic to decreased water resource. Similarly, at the northern margin, the pattern in the adjoining geomorphologically similar region consists of scattered shrub clusters, mainly associated with depressions and diffuse overland flow. The model suggests that this type of vegetation would differentiate into bands, provided that rainfall and topography are sufficient to generate uniform sheet flow. At both the arid and humid boundaries, the model tends to indicate that the patterns frequently regarded as degraded forms of '*brousse tigrée*' (White 1970) could equally be considered to be initial forms. With the alternating migrations of the climatic zones during the Quaternary, '*brousse tigrée*' patterns may have been initiated from humid mosaic patterns in some periods and from arid scattered shrub clusters in other periods. The model shows that the two common hypotheses about banding genesis, namely degradation of an initially uniform plant cover, or colonization of previously bare zones, correspond to two aspects of the same phenomenon rather than to distinct and contrary processes.

Whatever the initial conditions, banding occurs provided two conditions are met: (1) total rainfall is not sufficient to maintain a dense cover; (2) sufficient and uniform sheet flow can compensate, at least partly, for this lack of water. *Abiotic* (water resource) and *biotic* factors (competition and synergy) are sufficient for the model to simulate banding processes along contour lines and up-slope migration. This can originate from various initial vegetation arrangements, provided that a number of land, soil, and climatic conditions are met. Detailed studies of such feedbacks would lead to a better calibration of parameters for predicting ecological processes.

Although preliminary observations combined with literature data offer a good starting point to validate the model, additional studies are clearly needed, including run-off and soil moisture measurements. Furthermore, obtaining clear evidence to support the thesis that the bands migrate up-slope will require, besides the above successional studies, an array of various approaches including dendrochronology and soil isotopic analyses (Cs^{137}).

As illustrated by the model, bare patches which generate run-off are essential to supplement water (and possibly other resources) to the vegetation bands. Such a landscape patterning maximizes resource utilization and represent vegetation in dynamic equilibrium. Rehabilitation strategies should take into account this subtle hydrological balance in the banding patterns.

Acknowledgements

Thanks are due to M. Lepage for termite identification, to J. C. Menaut and G. Long for comments on a first draft of the paper, and to the scientific team of the ORSTOM centre of Niamey for helpful discussions in the field. This work was partially funded by the '*SAvanna on the Long Term (SALT)*' core-project of the Global Change Terrestrial Ecosystems project.

References

Ambouta, K. (1984) *Contribution à l'édaphologie de la brousse tigrée de l'ouest nigérien*. Thèse de Docteur Ingénieur, Université de Nancy.

Barker, T. (1992) *Vegetation pattern in the Nigerien tiger bush*. M. Sci., Coventry Polytechnic, Coventry, UK.

Boaler S.B. & Hodge, C.A.H. (1962) Vegetation bands in Somaliland. *Journal of Ecology*, **50**, 465–524.

Boaler, S.B. & Hodge, C.A.H. (1964) Observations on vegetation arcs in the northern region of the Somali Republic. *Journal of Ecology*, **52**, 511–544.

Boudet, G. (1972) Désertification de l'Afrique tropicale sèche. *Adansonia*, ser.**2**, **12**, **4**, 505–524.

Casenave, A. & Valentin, C. (1992) A run-off capability classification system based on surface features criteria in the arid and semi-arid areas of West Africa. *Journal of Hydrology*, **130**, 231–249.

Clos-Arceduc, M. (1956) Etude sur photographies aériennes d'une formation végétale sahélienne: la brousse tigrée. *Bulletin de l'IFAN, série A*, **7** (3), 677–684.

Conway, J.H. (1976) *On Numbers and Games*. Academic Press, London.

Cornet, A., Delhoume, J.P. & Montaña, C. (1988) Dynamics of striped vegetation patterns and water balance in the Chihuahuan desert. *Diversity and Pattern in Plant Communities* (eds H. J. During, M. A. Werger & H. J. Willems), pp. 221–231. SPB Academic Publishing, The Hague.

Cornet, A. Montaña, C., Delhoume, J.P. & Lopez-Portillo J. (1992) Water flows and the dynamics of desert vegetation stripes. *Landscape Boundaries Consequences for Biotic Diversity and Ecological Flows* (eds A. J. Hansen & F. di Castri), pp. 327–345. Ecological Studies, **92**. Springer Verlag, New-York.

Delahaye J-P. (1991) Les automates. *Pour la Science*, **169**, 129–134.

Gavaud, M. (1966) *Etude pédologique du Niger occidental*, Vol. 1–3. ORSTOM, Paris.

Goutorbe,J.P., Lebel,T., Tinga, A. *et al.* (1994) HAPEX-Sahel: a large-scale study of land atmosphere interactions in the semi-arid tropics. *Annales Geophysicae*, **12**, 53–64.

Hemming, C.F. (1965) Vegetation arcs in Somaliland. *Journal of Ecology*, **53**, 57–68.

Lebel, T., Sauvageot, H., Hoepffner, M., Desbois, M., Guillot, B. & Hubert, P. (1992) Rainfall estimation in the Sahel: the EPSAT-NIGER experiment. *Hydrological Sciences Journal*, **37** (3), 201–215.

Leprun, J.C. (1992) Etude de quelques brousses tigrées sahéliennes: structure, dynamique, écologie. *L'aridité, une contrainte au développement* (eds E. Le Floc'h, M. Grouzis, A. Cornet & J. C. Bille), pp. 221–244. ORSTOM, Coll. Didactiques, Paris.

Mabbutt, J.A. & Fanning P.C. (1987) Vegetation banding in arid western Australia. *Journal of Arid Environments*, **12**, 41–59.

Mauchamp, A., Rambal, S. & Lepart, J. (1994) Simulating the dynamics of a vegetation mosaic: a spatialized functional model. *Ecological Modelling*, **71**, 107–130.

Montaña, C., Lopez-Portillo J. & Mauchamp, A. (1990) The response of two woody species to the conditions created by a shifting ecotone in an arid ecosystem. *Journal of Ecology*, **78**, 789–798.

Montaña, C. (1992) The colonization of bare areas in two-phase mosaics of an arid ecosystem. *Journal of Ecology*, **80**, 315–327.

Serpantié, G., Tezenas du Montcel L. & Valentin, C. (1991) La dynamique des états de surface d'un territoire agro-pastoral soudano-sahélien sous aridification climatique: Conséquences et propositions. *L'aridité, une contrainte au développement* (eds E. Le Floc'h, M. Grouzis, A. Cornet, J. C. Bille), pp. 419–448. ORSTOM, Coll. Didactiques, Paris.

Thiéry, J.M. (1991) °*VOYONS*°, programme de simulations conversationnelles en Physico-chimie et en Agronomie. *Logiciels pour la Chimie* (eds N. Antonot, G-M. Côme, T. Gartiser, J. Guidon & E. Soulié), pp. 292–293. Soc. Fr. Chimie, Paris, Agence Nat. Logiciel, CNRS, Nancy, France.

Tongway, D.J. & Ludwig J.A. (1990) Vegetation and soil patterning in semi-arid mulga lands of Eastern Australia. *Australian Journal of Ecology*, **15**, 23–34

Valentin, C. & Bresson, L.M. (1992) Morphology, genesis and classification of surface crusts in loamy and sandy soils. *Geoderma*, **55**, 225–245.

Van der Meulen, F. & Morris, J.W. (1979) Striped vegetation patterns in a Transvaal savanna (South Africa). *Geo-Eco-Trop*, **3** (4), 253–266.

White, L.P. (1969) Vegetation arcs in Jordan. *Journal of Ecology*, **57**, 461–464.

White, L.P. (1970) '*Brousse tigrée*' patterns in southern Niger. *Journal of Ecology*, **58**, 549–553.

White, L.P. (1971) Vegetation stripes on sheet wash surfaces. *Journal of Ecology*, **59**, 615–622.

Wickens G.E. & Collier F.W. (1971) Some vegetation patterns in the Republic of Sudan. *Geoderma*, **6**, 43–59.

Wilding, L.P. & Daniels, R. (1989) Soil, Geomorphic relationships in the vicinity of Niamey, Niger. *TropSoils Bulletin*, **89–01**.

Worrall, G.A. (1959) The Butana grass patterns. *Journal of Soil Science*, **10**, 34–53.

Received 25 March 1994
Revised version accepted 12 September 1994